

# Organic & Biomolecular Chemistry

Accepted Manuscript



This article can be cited before page numbers have been issued, to do this please use: T. Govindaraju, M. Ramesh, P. Makam, C. Voshavar, H. Khare, K. Rajasekhar and S. ramakumar, *Org. Biomol. Chem.*, 2018, DOI: 10.1039/C8OB01691G.



This is an Accepted Manuscript, which has been through the Royal Society of Chemistry peer review process and has been accepted for publication.

Accepted Manuscripts are published online shortly after acceptance, before technical editing, formatting and proof reading. Using this free service, authors can make their results available to the community, in citable form, before we publish the edited article. We will replace this Accepted Manuscript with the edited and formatted Advance Article as soon as it is available.

You can find more information about Accepted Manuscripts in the [author guidelines](#).

Please note that technical editing may introduce minor changes to the text and/or graphics, which may alter content. The journal's standard [Terms & Conditions](#) and the ethical guidelines, outlined in our [author and reviewer resource centre](#), still apply. In no event shall the Royal Society of Chemistry be held responsible for any errors or omissions in this Accepted Manuscript or any consequences arising from the use of any information it contains.



Journal Name

ARTICLE

## L-Dopa and dopamine conjugated naphthalenediimides modulate amyloid $\beta$ toxicity

Madhu Ramesh,<sup>a,†</sup> Pandeewar Makam,<sup>a,†</sup> Chandrashekhar Voshavar<sup>a,†</sup> Harshavardhan Khare,<sup>b</sup> Kolla Rajasekhar,<sup>a</sup> Suryanarayanan Ramakumar,<sup>b</sup> Thimmaiah Govindaraju<sup>\*a</sup>

Received 00th January 20xx,  
Accepted 00th January 20xx

DOI: 10.1039/x0xx00000x

www.rsc.org/

The process of protein misfolding and aggregation to form neurotoxic species is strongly implicated in most of the neurodegenerative disorders. In particular, amyloid beta ( $A\beta$ ) misfolding and aggregation is central to pathophysiological processes of Alzheimer's disease. Development of aggregation modulators has enormous implications in the discovery of effective therapeutic agents for Alzheimer's disease. Herein, we report the design and synthesis of series of natural amino acids, L-dopa and dopamine appended derivatives of naphthalenediimide (NDI) to identify efficient aggregation modulators. Furthermore, the molecular docking studies revealed the possible binding sites and binding mode of NDI-conjugates to  $A\beta$  aggregates. Among the designed NDI-conjugates, L-dopa and dopamine derivatives (**NLD** and **NDP**, respectively) showed excellent aggregation modulation efficiency (inhibition and dissolution), as shown by the thioflavin T (ThT) binding assays, dot blot analysis and *in cellulo* studies. The docking results from *in silico* study are in good agreement with the experimental data. In addition to significant modulation efficiency towards  $A\beta$  aggregation, **NLD** and **NDP** possess antioxidant activity conducive to develop disease-modifying therapeutic agents for the treatment of Alzheimer's disease.

### Introduction

Alzheimer's disease (AD) is the most common neurodegenerative disorder worldwide, described by the progressive impairment of cognitive abilities leading to dementia and death.<sup>1</sup> The prevalence of AD increases with age and severely affects population over the age of 60 years. However, approximately 10-12% of population with the disease have early onset AD which often appears at the young age of 40-50.<sup>2</sup> It was estimated that 35.6 million people were suffering from dementia or related disorders worldwide in 2010 and projected to raise up to 70 and 135 million in 2030 and 2050, respectively. Neurodegeneration in hippocampus and cerebral cortex of the brain caused by extracellular senile plaques (SP) and intracellular neurofibrillary tangles (NFTs) is the cardinal feature of Alzheimer's disease.<sup>3,4</sup> The protein cleavage, misfolding, aggregation and depositions of the aforementioned aggregates trigger an array of pathological events ultimately leading to multifaceted neurotoxicity during AD progression.<sup>5,6</sup> Several hypotheses are proposed to understand the pathophysiology of AD and most of these

hypotheses centred around abnormal increase in the cerebral senile plaques.<sup>7</sup> The senile plaques predominantly consist of  $A\beta_{42}$  peptide and is considered to play pivotal role in causing multifaceted neuronal toxicity in the AD brain.<sup>8</sup> The degree of cognitive impairment in AD patients has been found to correlate well with  $A\beta$  accumulation in the brain.<sup>9,10</sup> Although few drugs have been approved in the past few decades for the treatment of AD condition, these drugs provide only symptomatic relief and do not prevent the disease progression.<sup>11</sup> The mechanism of action of these drugs is through modulation of signaling pathways (modulate concentration levels of specific neurotransmitters in the brain) to temporarily improve the memory and hence do not act on the core pathology of AD. As a consequence, currently there is an unmet need for the development of disease-modifying therapeutic agents for the treatment of AD. In principle, modulation of aggregation pathway is an attractive and promising approach to develop disease-modifying therapeutic agents.<sup>4</sup> In addition, design of small molecules that can target various pathological factors (multifunctional modulators) associated with the multifactorial disease processes is desirable.<sup>3,12-14</sup> There are several approaches to modulate AD pathology that include development of effective modulators of  $A\beta$  aggregation, antioxidants and metal chelators among others.<sup>15-17</sup> Despite the significant progress in the AD research, there are no effective approaches in designing multifunctional  $A\beta$  modulators.

Several polyphenolic compounds such as epigallocatechin gallate (EGCG), curcumin, resveratrol, ferulic acid and hypericin have shown disrupting effect on the  $A\beta$

<sup>a</sup> Bioorganic Chemistry Laboratory, New Chemistry Unit, Jawaharlal Nehru Centre for Advanced Scientific Research, Jakkur P.O., Bengaluru 560064, Karnataka, India.

<sup>b</sup> Department of Physics, Indian Institute of Science, Bengaluru-560012, India.

† These authors contributed equally.

\* Corresponding author Email: tgraju@jncasr.ac.in

Electronic Supplementary Information (ESI) available: [Synthesis procedure and characterisation data, ThT assay with  $A\beta_{11-25}$  peptide, detailed *in silico* docking protocols]. See DOI: 10.1039/x0xx00000x

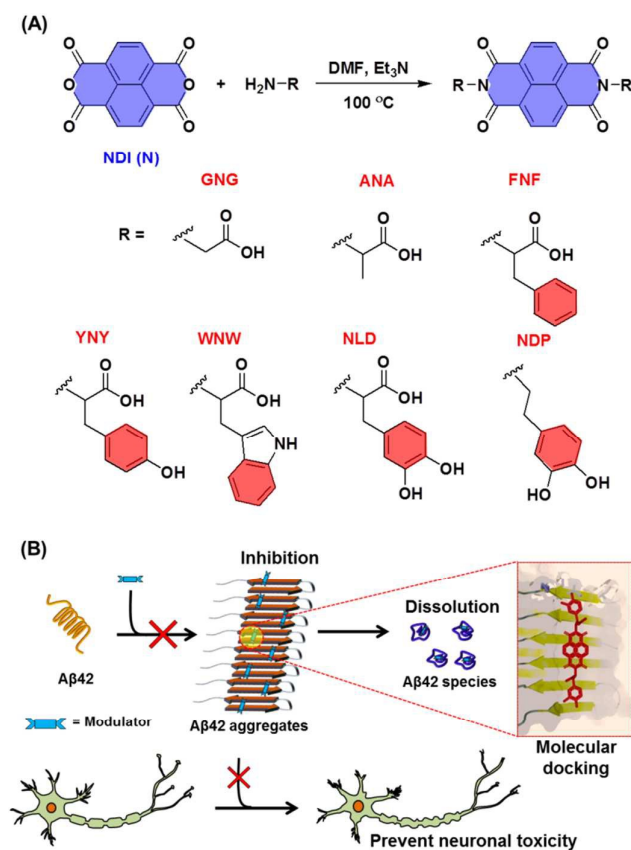


Fig. 1 (A) Synthetic scheme and chemical structure of NDI modulators. (B) Schematic representation for modulation of Aβ toxicity by NDI modulators.

aggregation.<sup>18</sup> These natural compounds are known to perturb the hydrophobic forces responsible for the formation of amyloid aggregates.<sup>13,19-24</sup> In addition, the polyphenolic compounds exhibit excellent antioxidant property, a desirable attribute necessary to modulate excessive reactive oxygen species (ROS), oxidative stress and biomolecule damage.<sup>16, 17, 25</sup> In this article, we report the design and synthesis of amino acids, L-dopa and dopamine functionalised NDIs and the detailed study to identify potential multifunctional modulator of amyloid toxicity under *in vitro* conditions. Various biophysical, *in vitro* and cell-based studies revealed that the L-dopa (**NLD**) and dopamine (**NDP**) conjugated NDIs effectively modulate Aβ<sub>42</sub>-aggregation and quench ROS, as a result these modulators rescue PC12 cells from multifaceted amyloid toxicity. Furthermore, the *in vitro* experimental results are supported by the molecular docking studies which revealed the interaction of **NLD** and **NDP** in KLVFFA, IIGLM regions of Aβ<sub>42</sub> with high binding affinities. Overall, these results clearly indicate the potential of **NLD** and **NDP** to effectively modulate Aβ<sub>42</sub> aggregation, oxidative stress and rescue PC12 cells from amyloid toxicity.

## Results and discussion

### Design and synthesis of NDI-conjugates

Targeting the hydrophobic pockets of Aβ aggregates through hydrophobic moieties has been the key strategy for developing aggregation modulators. This strategy prompted us to design series of compounds with variable chemical functional groups around a central hydrophobic aromatic core that can modulate Aβ aggregation. We selected naphthalene aromatic core of NDI as central hydrophobic moiety, to which chosen functional groups were conjugated (Fig. 1A). NDIs are thermally stable, planar π-electron deficient with well-defined redox and optical properties and as a consequence finds a wide range of applications from materials to biomedicine.<sup>26,27</sup> Analogous to aforementioned natural aromatic modulators, the planar and compact aromatic skeleton of NDI in the designed compounds is envisioned to modulate Aβ aggregation by interacting in the hydrophobic pockets of Aβ polymorphic species. Further, we assumed that the covalent functionalisation of NDI at imide position with amino acids having variable α-substituents and phenolic moieties can potentially yield active compounds with the ability to modulate Aβ aggregation process through various non-covalent interactions and armed with intrinsic antioxidant property. Accordingly, we conjugated NDI with various aliphatic and aromatic natural amino acids (glycine, alanine, tryptophan, phenylalanine and tyrosine in **GNG**, **ANA**, **WNW**, **FNF** and **YNY**, respectively). To introduce antioxidant property, NDI was conjugated with special amino acid L-dopa and dopamine as in **NLD** and **NDP**, respectively. Dopamine is a well-known neurotransmitter, which is structurally similar to L-dopa but lacks carboxylic acid group. Briefly, 1,4,5,8-naphthalenetetracarboxylic dianhydride was dispersed in dimethylformamide followed by the addition of triethylamine and amino acids under reflux conditions. The product was precipitated by acidifying the concentrated reaction mixture by the addition of 1N HCl. The precipitate was collected by filtration, washed with excess of distilled water and dried under vacuo to obtain the natural amino acids, L-dopa and dopamine conjugated NDIs (**ANA**, **GNG**, **YNY**, **WNW**, **FNF** and **NLD**) in good to excellent yields (70-90%) without the need of any further purification. For **NDP**, acidification step with HCl was excluded, the reaction mixture after DMF removal was added with water and directly filtered using buchner funnel. The precipitate was washed with copious amounts of water and dried under vacuo to obtain **NDP** in quantitative yield. All the compounds were characterised by NMR and high resolution mass spectrometry (HRMS) analysis.

### Modulation of Aβ<sub>11-25</sub> aggregation

The NDI conjugates were studied for inhibition and dissolution efficacies against Aβ<sub>11-25</sub> aggregation by ThT assay. Aβ<sub>11-25</sub> is a short hydrophobic fragment derived from Aβ<sub>42</sub>, which on incubation in PBS buffer (10 mM, pH 7.4) at 37 °C attains β-sheet conformation and form fibrillary aggregates similar to full length peptide (Aβ<sub>42</sub>). For the inhibition experiment, 200 μM of Aβ<sub>11-25</sub> was incubated without and with NDI conjugates at 1:1 ratio for 48 h. ThT fluorescence assay showed an intense fluorescence band at 482 nm for Aβ<sub>11-25</sub> (control) indicating the formation of amyloid fibrils (Fig. S1). In contrast, Aβ<sub>11-25</sub> incubated independently with **GNG** and

**ANA** showed slight decrease in fluorescence of ~44% and ~39% respectively, while compounds **FNF** (~85%) and **YNY** (~86%) caused five times decrease in the ThT fluorescence intensity compared to A $\beta$ 11-25 alone. Remarkably, **NLD** and **NDP** showed drastic decrease in fluorescence of 98% and 96%, respectively. (Fig. S1). The fluorescence intensity of ThT is directly correlated to the extent of amyloid aggregation and the observed loss of fluorescence in the presence of **NLD** and **NDP** is an indicative of inhibition of A $\beta$ 11-25 aggregation. Next, we performed dissolution of pre-formed A $\beta$ 11-25 fibrils in the presence of NDI conjugates. The A $\beta$ 11-25 pre-formed fibrils were incubated with NDI conjugates for 48 h at 37 °C and the change in ThT fluorescence was measured in comparison with untreated A $\beta$ 11-25 (Fig. S1). Interestingly, **NLD** and **NDP** treated samples exhibited significantly low fluorescence emission which is attributed to efficient dissolution of pre-formed A $\beta$ 11-25 fibrils. **FNF** and **YNY** showed ~5 and ~3 fold decrease in ThT fluorescence indicating the moderate dissolution efficiency (Fig. S1). **ANA** did not show any dissolution activity of pre-formed fibrils as indicated by the unperturbed intense fluorescence band at 482 nm. Based on this preliminary screening for dissolution of A $\beta$ 11-25 aggregates with different NDI conjugates, we performed time- and concentration-dependent studies with most effective NDI modulators (Fig. S2). In these experiments, each compound in selected concentrations (10, 25 and 50  $\mu$ M) was incubated with pre-formed fibrils prepared using A $\beta$ 11-25 fragment for 0, 1, 2, 3 and 6 days. The data from the ThT fluorescence measurements showed **NLD** and **NDP** are the most effective aggregation modulators and the dissolution efficiency towards A $\beta$ 11-25 fibrils was found to be in the order of **NLD** > **NDP** > **WNW** > **FNF** > **YNY**.

#### Modulation of A $\beta$ 42 aggregation

The promising results from the preliminary screening of NDI conjugates in modulating the A $\beta$ 11-25 aggregation encouraged us to evaluate their potential against A $\beta$ 42 aggregation. We performed a systematic study with active NDI modulators (**NLD**, **NDP**, **WNW** and **FNF**) along with inactive **ANA** (Fig. 2). In this experiment, 50  $\mu$ M of A $\beta$ 42 in PBS (10 mM, pH 7.4) was incubated alone or with 50  $\mu$ M of NDI conjugates in the presence of ThT for 24 h at 37 °C (Figure 2A). We found that compounds **NLD** and **NDP** showed highest inhibition (~90% and ~91% respectively) activities followed by **WNW** and **FNF** (55% and 45% respectively), while **ANA** did not show significant inhibition. Further, dot blot assay was performed to confirm the inhibition efficiency of NDI modulators observed in ThT assay. A $\beta$ 42 (10  $\mu$ M) was incubated independently with 10  $\mu$ M of **ANA**, **FNF**, **WNW**, **NLD** and **NDP** for 48 h at 37 °C. These samples were blotted on PVDF membrane and treated with OC primary antibody (binds to A $\beta$ 42 fibrillar aggregates) followed by the fluorescent secondary antibody (labelled with Alexa fluor-488).<sup>28</sup> The fluorescent intensity of A $\beta$ 42 treated with NDI-modulators was quantified in comparison to control (untreated A $\beta$ 42). This data revealed that **ANA** and **FNF** did not show any significant inhibition of A $\beta$ 42 aggregation (Figure 2B and C). Whereas, **WNW**, **NLD** and **NDP** showed inhibition

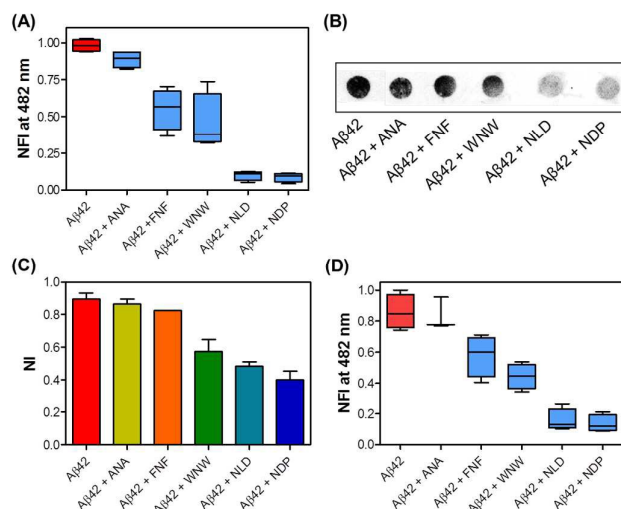


**Fig. 2** Inhibition and dissolution of A $\beta$ 42 aggregates by NDI modulators (**ANA**, **FNF**, **WNW**, **NLD** and **NDP**). (A) A $\beta$ 42 alone or with NDI modulators were incubated for 24 h at 20  $\mu$ M concentration at 1:1 ratio in PBS. (B) Dot blot analysis of A $\beta$ 42 (10  $\mu$ M) incubated with NDI modulators (10  $\mu$ M). (C) Quantification of dot blot. (D) Preformed A $\beta$ 42 aggregate (20  $\mu$ M) was incubated with NDI modulators at 20  $\mu$ M (at 1:1 molar ratio) for 48 h for dissolution assay. Values are the normalized maximal fluorescence intensity at 482 nm compared to that of the control (A $\beta$ 42 without NDI modulators).

efficiency of 40%, 50% and 60%, respectively. This data showed effective inhibitory effect of **NLD** and **NDP** towards A $\beta$ 42 aggregation and these findings are consistent with the ThT assay. Next, we performed concentration dependent inhibition of A $\beta$ 42 (50  $\mu$ M) aggregation using **NLD** and **NDP** at 1:1, 1:2 and 1:5 ratio of A $\beta$ 42 and **NLD/NDP** (Fig. S4). Both **NLD** and **NDP** showed good inhibition efficiency of 80% and 85%, respectively at 1:1 ratio. The percentage of inhibition efficiency reached >90% with increase in the ratio of NDI-modulator. Further, we analysed the A $\beta$ 42 aggregation in the absence and presence of lead NDI modulators (**NLD** and **NDP**) through transmission electron microscopy (TEM) analysis. The TEM data showed that both **NDP** and **NLD** effectively prevent the formation of A $\beta$ 42 fibrillar aggregates compared to control (A $\beta$ 42 formed fully grown aggregates in the absence of modulators) (Fig. S3).

Next, we evaluated the ability of **NLD**, **NDP**, **WNW** and **FNF** to dissolve the pre-formed A $\beta$ 42 fibrils by ThT fluorescence assay. In this assay, both **NLD** and **NDP** showed maximum dissolution ability of ~80%, while **WNW** and **FNF** exhibited moderate dissolution efficiency (~50% and 30%, respectively) of pre-formed fibrils (Fig. 2D). These findings are in good agreement with corresponding dissolution profiles obtained for A $\beta$ 11-25 aggregates. **ANA** did not show any significant effect on the fibrils, as the ThT fluorescence intensity remained unchanged and comparable to that of untreated A $\beta$ 42 fibrils. In order to understand the effect of concentration on dissolution ability, we performed concentration-dependent study with **NLD** and **NDP** (Fig. S4). The dissolution effects of **NLD** and **NDP** were found to be similar to the data from concentration-dependent inhibition of A $\beta$ 42 aggregation (50

$\mu\text{M}$ ) (Fig. S4). **NLD** showed relatively superior dissolution effect with increasing concentration ( $\sim 88\%$  at 1:1 ratio and  $\sim 93\%$  at 1:5 ratio) compared to **NDP** which exhibited dissolution

of **NDI** conjugates on docking to different regions of  $\text{A}\beta$  fibrils which is in agreement with the *in vitro* activity of the **NDI** modulators. In order to perform an unbiased search for

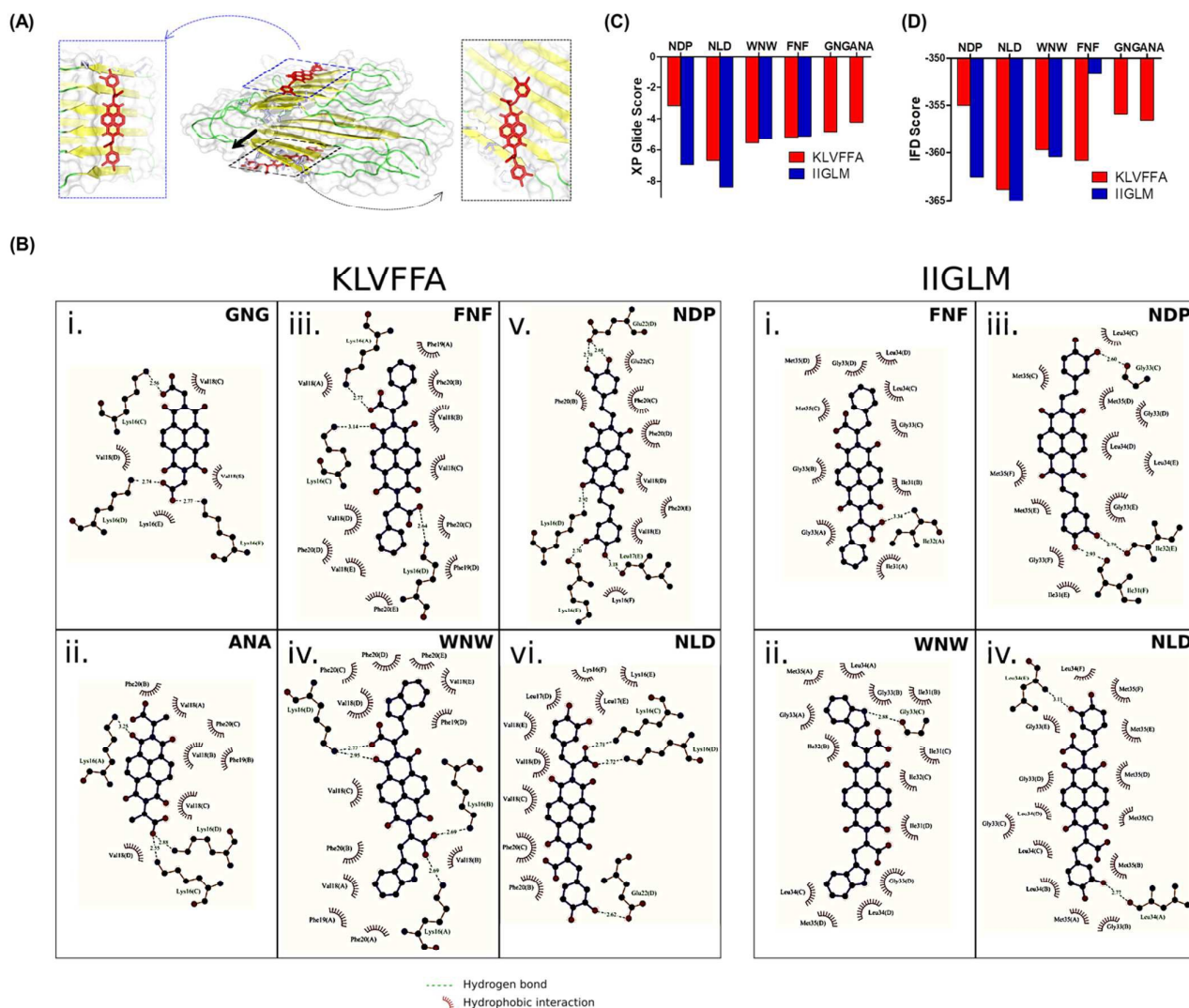


**Fig. 3** Docking scores for two binding regions (A). (B) Ligand interaction analysis of docked ligands to KLVFFA and IIGLM regions. KLVFFA region shows docked poses of all 6 ligands, whereas, IIGLM region does not show significant docking of **GNG** and **ANA**. (Figures generated using Ligplot+ Software). (C) XP Glide docking scores for the 6 ligands. (D) IFD docking scores for the 6 ligands. (C) and (D) show distinctly better docking scores of **NLD** for both KLVFFA and IIGLM regions

efficiency of  $\sim 85\%$  and  $\sim 95\%$  at treatment ratios of 1:1 and 1:5, respectively. Overall, the results from inhibition and dissolution experiments confirmed that **NLD** and **NDP** are the effective modulators of  $\text{A}\beta_{42}$  aggregation with former being marginally superior over the later.

#### Molecular docking studies

Understanding the binding mechanisms of amyloid modulators has been of interest for the rational design of small molecule inhibitors of  $\text{A}\beta$  aggregation.<sup>10,12,16,29</sup> There are reports that show ridges and grooves on  $\text{A}\beta$  fibrils serve as binding regions for ligands, especially the 'flat' ligands.<sup>30,29,31</sup> From this point of view, we investigated the mechanisms of groove binding using our rationally designed **NDI** conjugates with various functional groups. We show the correlation of various functional groups

possible binding sites for **NDI** conjugates on the  $\text{A}\beta$  surface, we adopted computational blind docking strategy followed by extra-precision and induced fit docking for selected sites (see ESI for detailed blind docking protocol). We used Glide program in Schrodinger Software Suite<sup>32-34</sup> for all the docking studies. In contrast to usual docking studies where the binding site is known, blind docking is an iterative method designed to uniformly scan the entire surface of the receptor. We automated this procedure through in-house written python scripts that generate an equi-spaced grid over the surface of the receptor and test the docking performance systematically at each grid point. However, this method involves large sampling time due to its inherent exhaustiveness and hence we opted for low precision (or standard precision) docking in this step. Based on the results from low precision blind docking

studies, we selected binding hot spots. Further, we performed extra precision (XP) docking and induced fit docking (IFD)<sup>35,36</sup> for the selected hot spots to understand the details of possible binding sites and the docked ligands.

Several structures have been proposed for A $\beta$  aggregates based on solid-state NMR experiments.<sup>37,38</sup> To select the receptors for docking studies, the A $\beta$  aggregate structures available in Protein Data Bank (PDB) were analysed in terms of experimental conditions and length of the peptide used. Although PDB ID 2BEG38 (Fig. S5) matched these two criteria, the structure is refined from Leu17 onwards and has only 5 refined chains which represent an insufficient length of binding groove for our ligands. However, there are other solid-state NMR structures of A $\beta$ 40 in PDB with 6 refined chains stacked over each other which give sufficiently long grooves on the surface. We verified and confirmed that the side chain orientations of these A $\beta$ 40 structures match with those observed in 2BEG (which is A $\beta$ 42). PDB IDs 2LMN, 2LMO are two such A $\beta$  fibril structures which have six refined chains (Fig. S4) and we have chosen 2LMO for our docking studies. Nevertheless, we performed docking with 2BEG and obtained similar docked poses but with lower docking scores which can be attributed to the missing hydrogen bonds as compared to the ligands docked to 2LMO. This result revealed that longer grooves (or binding sites) are necessary to obtain correctly docked poses of our NDI conjugates. Residue-wise C $\alpha$  RMSD (Root Mean Square Deviation) analysis for the NMR structures showed two regions viz., residues 13–22 and residues 29–38, with distinctly low RMSD values as compared to other regions in the selected receptor model sequences (Fig. S5). These two regions are the  $\beta$ -strand forming regions in the A $\beta$  sequence and have been consistently shown to form  $\beta$ -sheets in many fibril structures.<sup>37–40</sup> The low RMSD regions also include two sequence stretches, viz. A $\beta$ 16–20 (KLVFFA) and A $\beta$ 31–35 (IIGLM) that promote the formation of  $\beta$ -sheets in amyloid fibrils.<sup>40</sup>

Analysis of docked poses in the two low RMSD regions showed preferential binding of our NDI conjugates with varying degrees of docking scores and selectivity. Results of blind docking studies showed a correlation between the docked poses of the NDI conjugates and two key regions of A $\beta$  fibril model, namely KLVFFA and IIGLM. All NDI conjugates could be docked to KLVFFA region, whereas, IIGLM region did not show any docked poses of **ANA** and **GNG**. We have extended these results using XP and IFD to investigate the interactions of NDI conjugates in the two regions. For XP docking, we used rigid receptor and flexible NDI conjugate which showed highest docking score for **NLD** and **NDP** followed by **WNW** and **FNF** docked to IIGLM site, while there was a difference in the scores for KLVFFA site with **NLD** showing highest score followed by **FNF**, **WNW**, **ANA** and **GNG** (Fig. 3. and Table S1 and S2). Interestingly, **NDP** showed the least preference for binding interaction towards KLVFFA. Overall, XP docking results showed highest docking preference for **NLD** followed by **NDP** with a glide docking score of -8.37 kcal/mol and -6.95 kcal/mol, respectively for IIGLM site. **WNW** and **FNF** showed glide docking scores of -5.29 kcal/mol and -

5.09 kcal/mol, respectively for the same site, while **GNG** and **ANA** did not show any docked poses. For KLVFFA region, **NLD** showed the highest score of -6.67 kcal/mol followed by **WNW** (-5.56 kcal/mol). **FNF**, **ANA** and **GNG** showed -5.17, -4.81, -4.21 kcal/mol glide docking scores, respectively. **NDP** had an unexpectedly low score of -3.18 kcal/mol for KLVFFA (Fig. 3C). With the above results in hand, we further performed IFD analysis<sup>35,36</sup> wherein receptor was also made flexible in nature.

Table 1. Qualitative comparison of docking scores for ligands with respect to the functional groups

Observation	NDP	NLD, WNW	FNF	ANA, GNG
Docking score for IIGLM	High	High	Low	Avoid
Docking score for KLVFFA	Low	High	High	High
R group has carboxylic group	No	Yes	Yes	Yes
R group has aromatic ring	Yes	Yes	Yes	No
R group has H-bond donor on aromatic ring	Yes	Yes	No	No
R group size (Number of non-Hydrogen atoms)	10	13	11	4,5
Number of rotatable bonds in R group	3	4	4	2

The results were found to be similar compared to XP docking and are tabulated in Table S3 and S4. Preference of various NDI conjugates (as obtained from IFD) towards the two binding sites is compared in Fig. 3D.

#### NDI conjugates-receptor interaction analysis

NDI conjugates-receptor interaction analysis was performed to understand the effect of various functional groups on docking preferences of the NDI conjugates. The docking results showed different binding mechanisms adopted by various NDI conjugates based on the functional groups attached to NDI core. The correlation between the docking scores and the functional groups suggests a modular and combinatorial method for designing A $\beta$  inhibitors (Fig. 3B). The carboxylic groups of NDI modulators appeared to be important for binding of NDI conjugates to KLVFFA region suggesting their role in forming hydrogen bonds and salt bridges, specifically with lysine residues (Fig. 3B). **NDP** which lacks carboxylic functionality among all the NDI conjugates showed lowest IFD scores for KLVFFA region. On the other hand, the carboxylic groups do not seem to be involved in any hydrogen bond or salt bridge interaction in the IIGLM region. However, carboxylic groups might assist NDI conjugate binding by protecting the hydrophobic ligand-receptor interface from being exposed to the solvent. The influence of hydroxyl groups attached to the phenyl rings is more pronounced in NDI conjugates docked in IIGLM region. In general, the hydrogen bond donating potential on the aromatic rings of the side chains appears to make hydrogen bonds with A $\beta$  backbone. **FNF** showed considerably low docking scores in IIGLM region compared to **NLD**, **NDP** and **WNW** which have hydrogen bond donors on the

aromatic rings in the imide functional groups. In KLVFFA region the hydrogen bond donors of **NLD**, **NDP** and **WNW** form side chain hydrogen bonding interactions, however their contribution to docking scores appears to be masked by the dominating effect of carboxylic groups. In general, the hydrogen bond donors on the aromatic rings of the side chains of the imide functional groups seems to make hydrogen bonds with A $\beta$  backbone. The aromatic ring systems are also important for better docking as it was inferred from the poor docking scores for both **ANA** and **GNG** in KLVFFA region and no docking poses in IIGLM region. The results are qualitatively summarised in **Table 1** which shows the correlation of docking preferences of individual NDI conjugate. A closer look at **Table 1** shows that NDI conjugates with aromatic ring and hydrogen bond donating groups gave best docking scores (**NLD**, **WNW**, **NDP**) with maximum non-covalent interactions in KLVFFA and IIGLM regions of A $\beta$  fibrils. Interestingly, these *in silico* observations are in agreement with the experimental results which showed superior aggregation-modulation activity for **NLD**, **WNW** and **NDP**. From *in silico* and *in vitro* results, it can be generalised that compounds that have three main characteristics, viz., aromatic rings, hydrogen bond donating potential on the aromatic rings and the carboxylic groups, are likely to be the best A $\beta$ 42 aggregation modulators. NDI conjugates which showed poor docking scores for IIGLM and KLVFFA were found to be experimentally inactive in both inhibition and disaggregation of A $\beta$  aggregates. It is evident from the above results that various functional groups attached to the NDI core of individual compounds show different preferences based on their interaction potentials with the selected regions of aggregates. Although computational docking has certain limitations in accurately predicting the binding sites/regions, the results from both docking and *in vitro* experiments have converged to similar findings. Taken together, current investigation of a series of NDI conjugates with varying functionalities provided significant information on the characteristics of aggregation modulators and paves a new path for the design of novel NDI modulators through a combinatorial approach.

#### Antioxidant property of NDI modulators

Elevated levels of ROS aggravates A $\beta$  aggregation and vice versa which results in biomolecule damage and neuronal cell death.<sup>41</sup> Development of A $\beta$  modulators supplemented with antioxidant properties is one of the widely explored strategies towards AD treatment.<sup>16,17</sup> It is well-known that polyphenols and flavonoids based natural compounds show good antioxidant property.<sup>42</sup> The NDI modulators with L-dopa (**NLD**) and dopamine (**NDP**) closely resemble polyphenolic compounds in terms of their structure (hydroxyl groups on the aromatic ring), function as aggregation modulators and possibly provide antioxidant effect. Keeping this in mind, **NLD**, **NDP**, **WNW** and **ANA** were assessed for antioxidant property in DPPH free radical scavenging assay. In this experiment, **NLD**, **NDP**, **WNW** and **ANA** along with ascorbic acid as a positive

control were studied at varying concentrations (20-200  $\mu$ M). The results from this study showed potent free radical scavenging activity of **NLD** and **NDP** (>80% and ~70% respectively), while that of **WNW** and **ANA** was in the range of 20-25% (Fig. 4).

Ascorbic acid (0 to 250  $\mu$ M) showed highest antioxidant property with free radical scavenging potential of ~85% at the initial reading. At the same time point, activities of **NLD** and **NDP** (0 to 250  $\mu$ M) were 20-30% (Fig. 4). The positive control

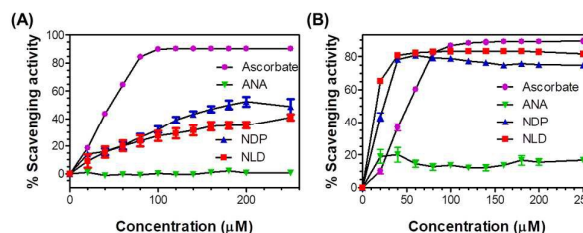


Fig. 4 DPPH free-radical scavenging (antioxidant) assay for **NLD**, **NDP**, **WNW**, **ANA** using Ascorbic acid as standard 0 h (A) and 2 h (B). Values shown are means  $\pm$  SEM of three independent experiments performed in three to four replicates. Radical scavenging activity was expressed as inhibition percentage and was calculated using the formula: % scavenging activity = (absorbance of control - absorbance of sample) / (absorbance of control)  $\times$  100.

ascorbic acid continued to show good radical scavenging activity (~80%) at 2 h and the activities of **NLD** and **NDP** were comparable at this point. Interestingly, **NLD** and **NDP** showed higher antioxidant property (~80%) at lower concentrations (< 50  $\mu$ M) while ascorbic acid exhibited ~35% activity at similar concentration (Fig. 4). These results suggested that **NLD** and **NDP** show steady and sustained antioxidant activity compared to ascorbic acid at lower concentrations. On the other hand, the observed low antioxidant property of **WNW** and **ANA** is due to absence of phenolic hydroxyl groups. Overall, **NLD** and **NDP** showed good antioxidant activity which may play key role in reducing the oxidative burden caused by ROS and prevent the progression of multifaceted A $\beta$  aggregation process.

#### A $\beta$ 42 aggregates induced toxicity in neuronal cells

After successfully establishing the modulation effects of NDI conjugates, we next sought to evaluate the effect of lead modulators **NLD** and **NDP** *in cellulo* conditions. First, the cytotoxic effects of pre-formed A $\beta$ 42 aggregates was assessed in pheochromocytoma cells (PC12) of the rat adrenal medulla. PC12 cell lines are neuroblastic cells and a good model for neuronal cells.<sup>43</sup> In this experiment, A $\beta$ 42 (100  $\mu$ M) in PBS (10 mM, pH 7.4) was incubated for 24 h at 37  $^{\circ}$ C to obtain A $\beta$ 42 fibrillar aggregates. PC12 cells were treated with preformed A $\beta$ 42 aggregates at variable concentrations (10, 7.5, 5, 2.5 and 1  $\mu$ M) for 24 h (Fig. S6). The main objective of this experiment was to determine the optimal concentration of A $\beta$ 42 aggregates that cause ~50% cell death. The cell viability of PC12 cells after A $\beta$ 42 treatment was accessed through MTT assay. Concentration dependent toxicity was observed in the PC12 cells with 1-10  $\mu$ M of A $\beta$ 42 aggregates exhibiting ~ 55-70% cytotoxic effect. Based on this study, 1  $\mu$ M of A $\beta$ 42 exhibiting 45% cell viability (55% cytotoxicity) was considered optimum for further experiments.

**NLD and NDP rescue neuronal cells from A $\beta$ 42 toxicity**

We assessed the ability of **NLD** and **NDP** to ameliorate the cytotoxicity induced by A $\beta$ 42 aggregates in PC12 cells. PC12 cells treated with aggregates prepared from 1  $\mu$ M concentration of A $\beta$ 42 showed ~55% cytotoxicity similar to the toxicity profile obtained in concentration-dependent study (Fig. 5A). The cells co-incubated with **NLD** (1  $\mu$ M) and A $\beta$ 42 (1

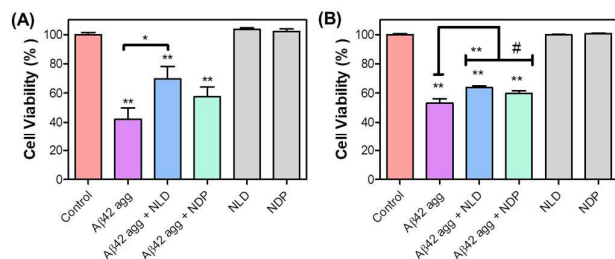


**Fig. 5.** *In vitro* studies with A $\beta$ 42 and NDI modulators **NLD** and **NDP**. (A) The effect of NDI modulators, **NLD** and **NDP** against A $\beta$ 42 aggregates on the cell viabilities of PC12 cells. A $\beta$ 42 either alone or with **NLD**, **NDP** are incubated for 24 h at 100  $\mu$ M concentration at 1:1 ratio in PBS. PC12 cells were treated with 1  $\mu$ M (final concentration per well w.r.t either A $\beta$  or drug) above samples for 24 h and assayed by MTT. (B) The effect of NDI modulators, **NLD** and **NDP** in disaggregation of pre-formed A $\beta$ 42 aggregates on the cell viabilities of PC12 cells. 200  $\mu$ M of A $\beta$ 42 alone in PBS was incubated for 24h followed by co-incubation with **NLD**, **NDP** for another 48 h at 100  $\mu$ M concentration at 1:1 ratio in PBS. PC12 cells were treated with 1  $\mu$ M (final concentration per well w.r.t either A $\beta$  or drug) above samples for 24 h and assayed by MTT. One-way ANOVA analysis followed by Tukey's multiple comparison post hoc test was performed (\*\* $p$  < 0.001 compared to control in a, b & c; \*\* $p$  < 0.001, \* $p$  < 0.01 and # $p$  < 0.05 compared to A $\beta$ 42 aggregates group in A & B).

$\mu$ M) aggregates showed a significant reduction in cell death (~30%), while **NDP** showed ~20% reduction (Figure 5A). The improved cell viability exhibited by **NLD** and **NDP** can be attributed to their anti-aggregation and antioxidant (phenolic groups) properties. Notably, **NLD** showed relatively superior cell viability against toxicity induced by A $\beta$ 42 aggregates compared to **NDP**. At this point, mechanism of action of **NLD** and **NDP** responsible for the observed inhibitory activities was not fully understood. The only structural difference between **NLD** and **NDP** is the presence of carboxylic acid functionality in the former which seems to play key role in the improved cell viability. We attempted to explain the observed modulation data and the possible role of carboxylic acid functionality of **NLD** in enhancing the activity, by performing docking studies. The carboxylic group of NDI modulators play a vital role in interaction with KLVFFA region through hydrogen bonding and salt bridge formation with the lysine residues of KLVFFA region, thus improving binding affinity. **NDP** lack carboxylic group, which has hampered its strong binding towards KLVFFA region leading to lower aggregation modulation efficiency and cell viability over **NLD**.

Next, we assessed the ability of **NLD** and **NDP** to modulate the pre-formed toxic aggregates in dissolution (disaggregation) experiments (Fig. S7). First, A $\beta$ 42 (200  $\mu$ M) was subjected to aggregation for 24 h followed by co-incubation with **NLD** and **NDP** at 100  $\mu$ M concentration (at 1:0.5 ratio) for 48 h. The

PC12 cells were treated with A $\beta$ 42 (1  $\mu$ M):**NLD**/**NDP** (1  $\mu$ M) for 24 h at 37  $^{\circ}$ C (Fig. 5B). The cells treated with A $\beta$ 42 aggregates showed ~50% cell death, while the cells co-incubated with A $\beta$ 42 aggregates and **NLD** showed only 35% cell death, a significant reduction in cell death by ~15% (Fig. 5B). **NDP** also showed a significant reduction in cell death by ~10% and slight reduction in the rescue activity could be attributed to the absence of carboxylic group compared to **NLD**. Thus, **NLD** is the most potent NDI modulator for rescuing neuronal cells from A $\beta$ 42 toxicity through both aggregation inhibition and dissolution of pre-formed A $\beta$ 42 aggregates.

**Conclusions**

In conclusion, we have developed natural amino acids, L-dopa and dopamine conjugated NDIs with dual functionality viz., modulation of A $\beta$ 42 aggregation and antioxidant property. ThT fluorescence assay and dot blot analysis revealed that **NLD** with L-dopa is an efficient modulator of A $\beta$ 42 aggregation and rescue neuronal cells from A $\beta$ 42 toxicity. *In silico* molecular docking results are found to be consistent with the *in vitro* and *in cellulo* studies. The molecular docking study showed the presence of hydrogen bonding and hydrophobic interactions of **NLD** in the hydrophobic pockets of A $\beta$ 42 aggregates, which is attributed to its efficient modulation of A $\beta$ 42 aggregation. Furthermore, the excellent antioxidant property of **NLD** as studied by the antioxidant scavenging assay, significantly contribute towards the rescue of neuronal cells from A $\beta$ 42 induced oxidative stress. Overall, the strategic design and easy access to NDI conjugates through simple synthetic routes and their activity-evaluation through various *in vitro*, *in silico* and *in cellulo* studies revealed **NLD** as a potent modulator of multifaceted A $\beta$ 42 toxicity.

**Experimental section****Materials**

PC12 Adh cells (a rat adrenal pheochromocytoma cell line) were kind gift from Dr. Praveen Vemula laboratory, INSTEM, NCBS, Bengaluru. Roswell Park Memorial Institute (RPMI) 1640 media, heat-inactivated horse serum, fetal bovine serum, penicillin-streptomycin and trypsin were purchased from Gibco (Grand Island, NY, USA). A $\beta$ 42 peptide was purchased from Calbiochem, Merck. Rink amide resin, Fmoc-amino acids were purchased from Novabiochem, USA. Dimethyl sulfoxide, methyl thiazolyl blue tetrazolium bromide (MTT), Dulbecco's phosphate-buffered saline (PBS) were purchased from Sigma-Aldrich. Dimethyl formamide and isopropanol were purchased from Acros Organics. DIPEA, HBTU, piperidine were purchased from Spectrochem, India. All the other chemicals and reagents were used as received unless otherwise mentioned.

**General procedure for the synthesis of amino acid and dopamine conjugated NDIs (GNG, YNY, NLD and NDP)**

1,4,5,8- Naphthalenetetracarboxylic dianhydride (NDA) (0.5 g, 1.8 mmol) and corresponding amino acid/dopamine (3.7 mmol) were suspended in 10 mL of dimethylformamide (DMF).

To this suspension, triethylamine (TEA) (0.2 mL) was added and allowed to reflux for 12 h. After cooling to room temperature and DMF was removed under high vacuum. The reaction mixture was added with 500 mL of 2N hydrochloric acid (HCl) and was stirred for 1 h. The precipitate was collected through buchner funnel attached with suction, washed with excess of distilled water (to remove excess HCl and other starting materials) and dried under vacuo to obtain amino acid-naphthalenediimide (NDI) conjugates (**GNG**, **YNY**, **NLD**) in quantitative yield. For **NDP**, acidification step with HCl was excluded. The reaction mixture after DMF removal was added with water and directly filtered using buchner funnel and precipitate was washed with water several times and the product was dried to obtain **NDP** in quantitative yield. Synthesis of **ANA**, **FNF** and **WNW** was reported in our earlier publication.<sup>44</sup> All the products were thoroughly characterised by NMR and mass spectrometry.

**GNG**: Yield: 70%; <sup>1</sup>H NMR (DMSO-d<sub>6</sub>, 400 MHz) δ<sub>H</sub> 13.20 (2H, b), 8.74 (4H, s), 4.77 (4H, s); <sup>13</sup>C NMR (DMSO-d<sub>6</sub>, 100 MHz) δ<sub>C</sub> 168.9, 162.2, 130.9, 126.2, 126, 41.5; HRMS: found 382.0437 [M+H]<sup>+</sup>, calcd. 382.0437 for [C<sub>18</sub>H<sub>10</sub>N<sub>2</sub>O<sub>8</sub>+H].

**YNY**: Yield: 75%; <sup>1</sup>H NMR (DMSO-d<sub>6</sub>, 400 MHz) δ<sub>H</sub> 12.99 (2H, b), 9.04 (2H, s), 8.65 (4H, s), 6.94 (J=1.15, 4H, d), 6.49 (J=1.72, 4H, t), 5.78 (J=2.55, 2H, q), 3.48 (2H, m), 3.24 (2H, m); <sup>13</sup>C NMR (DMSO-d<sub>6</sub>, 100 MHz) δ<sub>C</sub> 170.2, 161.8, 155.5, 131.1, 129.7, 127.6, 125.9, 125.5, 114.9, 54.7, 33.2; HRMS: found 595.1397 [M+H]<sup>+</sup>, calcd. 594.1274 for [C<sub>32</sub>H<sub>22</sub>N<sub>2</sub>O<sub>10</sub>+H]<sup>+</sup>.

**NLD**: Yield: 75%; <sup>1</sup>H NMR (DMSO-d<sub>6</sub>, 400 MHz) δ<sub>H</sub> 12.98 (2H, s), 8.66 (4H, s), 8.61 (2H, br), 8.52 (2H, br), 6.53-6.35 (8H, m), 5.74 (2H, q), 3.38 (2H, dd), 3.16 (2H, dd); <sup>13</sup>C NMR (DMSO-d<sub>6</sub>, 100 MHz) δ<sub>C</sub> 170.3, 161.9, 144.7, 143.5, 131.2, 128.4, 126.0, 125.6, 119.6, 116.2, 115.3, 54.8, 33.5; HRMS: found 627.1248 [M+H]<sup>+</sup>, calcd. 627.1246 for [C<sub>32</sub>H<sub>22</sub>N<sub>2</sub>O<sub>12</sub>+H].

**NDP**: Yield: 75%; <sup>1</sup>H NMR (DMSO-d<sub>6</sub>, 400 MHz) δ<sub>H</sub> 8.81 (2H, s), 8.67 (2H, s), 8.65 (4H, s), 6.68-6.62 (4H, m), 6.50 (2H, q), 4.17 (2H, dd), 2.75 (2H, dd); <sup>13</sup>C NMR (DMSO-d<sub>6</sub>, 100 MHz) δ<sub>C</sub> 162.3, 145.1, 143.7, 130.3, 129.2, 126.1, 125.9, 119.2, 115.9, 115.6, 41.7, 32.7; HRMS: found 539.1451 [M+H]<sup>+</sup>, calcd. 539.1449 for [C<sub>30</sub>H<sub>22</sub>N<sub>2</sub>O<sub>8</sub>+H].

#### Cell culture and treatments

PC12 Cells were cultured in T-75 flasks (Nest, India) and maintained in RPMI 1640 medium supplemented with 10% heat-inactivated horse serum, 5% fetal bovine serum, 100 U/mL penicillin, and 100 µg/mL streptomycin at 37 °C in 95% air/ 5% CO<sub>2</sub>. Stock solutions of **NLD** (10 mM) and **NDP** (10 mM) were prepared in dimethylsulfoxide (DMSO) and aliquots were stored at -20 °C. For all experiments assessing protective effects of **NLD** and **NDP**, PC12 cells were pre-treated with indicated concentrations of compounds for 24 h and then assayed for MTT unless stated otherwise. Controls were treated with media containing 0.01% DMSO.

#### Aggregation inhibition studies

Aβ<sub>11-25</sub> (see ESI for synthetic details) or Aβ<sub>42</sub> peptide (0.25 mg) (Calbiochem, Merck, USA) were dissolved in hexafluoro-2-propanol (HFIP, 0.2 mL) were incubated at room temperature for 1 h. HFIP was then removed by the thin flow of nitrogen

and further dried under vacuum. HFIP-treated Aβ<sub>11-25</sub> or Aβ<sub>42</sub> was then dissolved in PBS buffer to a final concentration of 100 µM at pH 7.4 and vortexed for approximately 30 s. NDI conjugates were dissolved in PBS buffer to a final concentration of either 200 µM or 100 µM. For inhibition studies involving Aβ<sub>11-25</sub>, 100 µM peptide was either added to the NDI conjugates at 1:1 ratio or incubated alone for 48 h at 37 °C. For studies involving inhibition of Aβ<sub>42</sub> aggregation, Aβ<sub>42</sub> (50 µM) was either added to NDI conjugates at 1:1 ratio or incubated alone for 24 h at 37 °C. Samples from each experiment were analysed by standard ThT fluorescence assay.

#### Aggregates dissolution studies

Aβ<sub>11-25</sub> or Aβ<sub>42</sub> peptide in PBS were dissolved to a final concentration of 200 or 100 µM and incubated for 24 or 48 h at 37 °C for the formation of aggregates/fibrils respectively for each peptide. For dissolution studies involving Aβ<sub>11-25</sub>, the peptide at 200 µM was incubated for 48 h followed by co-incubation with NDI conjugates for another 24 h or for 6 days (for time and dose dependent study) at 100 µM final concentrations (1:1 ratio). For control, 100 µM Aβ<sub>11-25</sub> was incubated alone for 72 h. Dissolution studies with Aβ<sub>42</sub>, 100 µM of peptide was initially incubated for 24 h followed by co-incubation with NDI conjugates for another 48 h at 50 µM final concentration (1:1 ratio). For control, 50 µM Aβ<sub>11-25</sub> was incubated alone for 72 h. Disaggregation of pre-formed fibrils in the presence of NDI conjugates was studied by ThT fluorescence assay.

#### ThT assay (Fluorescence spectroscopy)

Fluorescence spectral measurements were carried out using Perkin Elmer Model LS 55 fluorescence spectrophotometer. Maximum fluorescence of ThT was observed with the excitation and emission wavelengths set to 450 and 482 nm, respectively. A ThT concentration of 5-10 µM was used for Aβ<sub>42</sub> fibrillation and dissolution assays based on the fibrillar concentration.

#### Transmission Electron Microscopy (TEM)

The samples of Aβ<sub>42</sub> aggregates or Aβ<sub>42</sub>-modulator (**NDP** or **NLD**) were diluted to 5 µM in milliq water. Then 5 µL of each sample was adsorbed onto 200-mesh TEM grids for 10 min and washed for 1 min with distilled water. The samples were stained with uranyl acetate (2%) for 5 min and washed for 3 times with distilled water. The samples were dried overnight and visualised under TEM operating at 120 kV.

#### Molecular docking

The Glide program in Schrödinger Software Suite was used for all the docking studies. The general pipeline for docking used in this work is as shown in ESI. In order to perform an unbiased search for possible binding sites for NDI conjugates on the Aβ surface, we adopted computational blind docking strategy followed by extra-precision and induced fit docking for selected sites (see ESI for detailed blind docking protocol). Since the ligands in this study were new ligands, it was necessary to confirm the favourable binding regions using blind docking. In contrast to usual docking studies where the

binding site is known, blind docking is an iterative method designed to scan the whole surface of the receptor uniformly. This procedure was automated through in-house python scripts that generate an equispaced grid over the surface of the receptor and test the docking performance at each grid point systematically. However, this method involves large sampling due to its inherent exhaustiveness. Hence, low precision (or standard precision) docking (available in Glide program provided in Schrödinger Software Suite) was performed in this step. Based on the results from low precision blind docking studies, binding hot spots were selected. Extra precision (XP) docking and induced fit docking (IFD) were performed subsequently for the selected hot spots to understand the details of the docked poses of the ligands. Protocol for blind docking is given in the supplementary information.

#### DPPH radical scavenging assay (Antioxidant activity)

To a 96-well plate, 100  $\mu$ L aliquot of solution of NDI modulator (dissolved in methanol) ranging from 250 to 20  $\mu$ M was added. Next 100  $\mu$ L of 200  $\mu$ M methanolic solution of 1,1-DPPH was added, and the plate was shaken at 30  $^{\circ}$ C for 30 min. Control wells received 100  $\mu$ L of methanol and 100  $\mu$ L of 200  $\mu$ M methanolic DPPH solution. Wells containing only 200  $\mu$ L of methanol served as a background correction. The change in absorbance of all samples and standard (ascorbic acid) was measured at 517 nm. Absorbance was measured at every 30 min. For 0 min, absorbance was measured immediately after addition of DPPH solution. Radical scavenging activity was expressed as inhibition percentage and was calculated using the following formula:

$$\% \text{ scavenging activity} = \frac{(\text{absorbance of control} - \text{absorbance of sample})}{(\text{absorbance of control})} \times 100.$$

#### Cytotoxicity of A $\beta$ 42 aggregates in PC12 cells

A $\beta$ 42 peptide was dissolved in PBS buffer to a final concentration of 50  $\mu$ M and incubated at 37  $^{\circ}$ C for 24 h. The samples from 24 h incubation were used to evaluate the effect of various A $\beta$ 42 aggregation species on the viability of PC12 cells (extracellular toxicity). Briefly, PC12 cells were seeded at 17,000 cells/well density in 100  $\mu$ L of the medium in a 96-well plate. Cells were allowed to adhere to the plate for 24 h. 24  $\mu$ L (100  $\mu$ M, A $\beta$ 42) sample was diluted with PC12 cell medium to prepare variable concentrations of A $\beta$ 42 (1, 2.5, 5, 7.5, and 10  $\mu$ M) for cell culture experiments. Media was removed, and the adhered PC12 cells were treated with 60  $\mu$ L of A $\beta$ 42 (1-10  $\mu$ M) containing medium. For evaluating the effect of A $\beta$ 42 + NDI modulator, samples were diluted with PC12 medium to get the final concentration of A $\beta$ 42 and compound to 10  $\mu$ M in PC12 medium. Control cells were treated with appropriately diluted PC12 medium with PBS. Treatment with extracellular A $\beta$ 42 was conducted for 24 h. After incubation, 6  $\mu$ L of 5 mg/mL MTT was added to the cells and the plate was incubated for another 4 h at 37  $^{\circ}$ C under 5% CO<sub>2</sub> atmosphere. Next, the plate was centrifuged at 1500 rpm for 10 min and the supernatants were carefully removed. The formazan crystals were dissolved in 100  $\mu$ L of 1:1 mixture of DMSO/methanol solution by shaking gently at 400 rpm for 30 min at room temperature. Then the

absorbance was measured at 570 and 690 nm using microplate reader (Spectramax i3x, Molecular device). Background-corrected values (570–690 nm) were used to plot the graph. Data from at least three experiments were analysed using GraphPad software.

#### Modulation of A $\beta$ 42 toxicity in PC12 cells

A $\beta$ 42 alone (10  $\mu$ M) was able to induce around ~60% cell death after incubating for 24 h. Therefore, we assessed the ability of active NDI modulators, **NLD** and **NDP** to ameliorate the cytotoxicity induced by A $\beta$ 42 (10  $\mu$ M) after incubating for 24 h. The ability of NDI modulators to disaggregate the pre-formed fibrils was evaluated by the treatment of PC12 cells with **NLD** and **NDP**, for protective effects. For these experiments, A $\beta$ 42 was incubated with/without NDI modulator either in monomeric form (aggregation inhibition) or pre-formed aggregates (dissolution of aggregates). For aggregation inhibition experiment, 50  $\mu$ L of A $\beta$ 42 (100  $\mu$ M) was mixed with 50  $\mu$ L of NDI modulator (100  $\mu$ M) to yield 50  $\mu$ M final concentration, vortexed for approximately 30 s and incubated for 24 h at 37  $^{\circ}$ C. For dissolution experiment, pre-formed A $\beta$ 42 aggregates from 24 h incubation were further incubated either alone or with 100  $\mu$ M of NDI modulator for another 48 h. These samples were treated to PC12 cells at 1  $\mu$ M final concentration (A $\beta$ 42: NDI modulator) in DMEM complete media for 24 h. After 24 h of incubation, MTT assay was performed as mentioned above to assess the protective effects of NDI modulators.

#### Statistical analysis

Experimental data presented is the mean  $\pm$  SD of at least three independent experiments performed with 4–5 replicates. One-way ANOVA analysis followed by Tukey's multiple comparison post hoc test was performed. Data were compared among the different groups for individual experiment and  $p < 0.05$  was considered as significant.

#### Conflicts of interest

There are no conflicts to declare.

#### Acknowledgements

We thank Prof. C. N. R. Rao FRS for constant support and encouragement, JNCASR, SwarnaJayanti Fellowship, the Department of Science and Technology (DST), Government of India (Grant: DST/SJF/CSA-02/2015-2016) and Sheikh Saqr Laboratory (SSL), ICMS-JNCASR, for financial support.

#### References

1. M. Prince, R. Bryce, E. Albanese, A. Wimo, W. Ribeiro and C. P. Ferri, *Alzheimers Dement.*, 2013, **9**, 63-75.e62.
2. X.-C. Zhu, L. Tan, H.-F. Wang, T. Jiang, L. Cao, C. Wang, J. Wang, C.-C. Tan, X.-F. Meng and J.-T. Yu, *Ann. Transl. Med.*, 2015, **3**, 38.
3. Y. Huang and L. Mucke, *Cell*, 2012, **148**, 1204-1222.

## ARTICLE

## Journal Name

4. K. Rajasekhar, M. Chakrabarti and T. Govindaraju, *Chem. Commun.*, 2015, **51**, 13434-13450.
5. D. J. Selkoe, *Nature*, 2003, **426**, 900.
6. T. P. J. Knowles, M. Vendruscolo and C. M. Dobson, *Nat. Rev. Mol. Cell Biol.*, 2014, **15**, 384.
7. I. W. Hamley, *Chem. Rev.*, 2012, **112**, 5147-5192.
8. E. Karran, M. Mercken and B. D. Strooper, *Nat. Rev. Drug Discov.*, 2011, **10**, 698.
9. J. Näslund, V. Haroutunian, R. Mohs and et al., *JAMA*, 2000, **283**, 1571-1577.
10. Q. Nie, X.-g. Du and M.-y. Geng, *Acta Pharmacol. Sin.*, 2011, **32**, 545-551.
11. K. Rajasekhar and T. Govindaraju, *RSC Adv.*, 2018, **8**, 23780-23804.
12. F. Re, C. Airoidi, C. Zona, M. Masserini, B. L. Ferla and N. Q. a. F. Nicotra, *Curr. Med. Chem.*, 2010, **17**, 2990-3006.
13. S.-J. Hyung, A. S. DeToma, J. R. Brender, S. Lee, S. Vivekanandan, A. Kochi, J.-S. Choi, A. Ramamoorthy, B. T. Ruotolo and M. H. Lim, *Proc. Natl. Acad. Sci. USA.*, 2013, **110**, 3743-3748.
14. C. A. B., T. O. Laia, E. Alba, V. Guillem, N. Ernesto, S. Raimon and G. Patrick, *Chem. Eur. J.*, 2016, **22**, 7268-7280.
15. S. Pellegrino, N. Tonalì, E. Erba, J. Kaffy, M. Taverna, A. Contini, M. Taylor, D. Allsop, M. L. Gelmi and S. Ongeri, *Chem. Sci.*, 2017, **8**, 1295-1302.
16. K. Rajasekhar, K. Mehta and T. Govindaraju, *ACS Chem. Neurosci.*, 2018, **9**, 1432-1440.
17. K. Rajasekhar, C. Madhu and T. Govindaraju, *ACS Chem. Neurosci.*, 2016, **7**, 1300-1310.
18. D. R. Galasko, E. Peskind, C. M. Clark, J. F. Quinn, J. M. Ringman, G. A. Jicha, C. Cotman, B. Cottrell, T. J. Montine, R. G. Thomas and P. Aisen, *Arch. Neurol.*, 2012, **69**, 836-841.
19. F. Yang, G. P. Lim, A. N. Begum, O. J. Ubeda, M. R. Simmons, S. S. Ambegaokar, P. P. Chen, R. Kaye, C. G. Glabe, S. A. Frautschy and G. M. Cole, *J. Biol. Chem.*, 2005, **280**, 5892-5901.
20. D. E. Ehrnhoefer, J. Bieschke, A. Boeddrich, M. Herbst, L. Masino, R. Lurz, S. Engemann, A. Pastore and E. E. Wanker, *Nat. Struct. Mol. Biol.*, 2008, **15**, 558-566.
21. P. Marambaud, H. Zhao and P. Davies, *J. Biol. Chem.*, 2005, **280**, 37377-37382.
22. E. Bramanti, F. Lenci and A. Sgarbossa, *Eur. Biophys. J.*, 2010, **39**, 1493-1501.
23. Y. Porat, A. Abramowitz and E. Gazit, *Chem. Biol. Drug Des.*, 2006, **67**, 27-37.
24. A. Frydman-Marom, A. Levin, D. Farfara, T. Benromano, R. Scherzer-Attali, S. Peled, R. Vassar, D. Segal, E. Gazit, D. Frenkel and M. Ovdia, *PLoS One.*, 2011, **6**, e16564.
25. C. Cheignon, M. Tomas, D. Bonnefont-Rousselot, P. Faller, C. Hureau and F. Collin, *Redox Biol.*, 2018, **14**, 450-464.
26. M. B. Avinash and T. Govindaraju, *Adv. Mater.*, 2012, **24**, 3905-3922.
27. M. B. Avinash and T. Govindaraju, *Acc. Chem. Res.*, 2018, **51**, 414-426.
28. K. Rajasekhar, S. N. Suresh, R. Manjithaya and T. Govindaraju, *Sci. Rep.*, 2015, **5**, 8139.
29. G. Kuang, N. A. Murugan, Y. Tu, A. Nordberg and H. Ågren, *J. Phys. Chem. B*, 2015, **119**, 11560-11567.
30. L. Jiang, C. Liu, D. Leibly, M. Landau, M. Zhao, M. P. Hughes and D. S. Eisenberg, *eLife*, 2013, **2**, e00857.
31. G. Eskici and M. Gur, *PLoS One.*, 2013, **8**, e66178.
32. R. A. Friesner, R. B. Murphy, M. P. Repasky, L. L. Frye, J. R. Greenwood, T. A. Halgren, P. C. Sanschagrin and D. T. Mainz, *J. Med. Chem.*, 2006, **49**, 6177-6196.
33. T. A. Halgren, R. B. Murphy, R. A. Friesner, H. S. Beard, L. L. Frye, W. T. Pollard and J. L. Banks, *J. Med. Chem.*, 2004, **47**, 1750-1759.
34. R. A. Friesner, J. L. Banks, R. B. Murphy, T. A. Halgren, J. J. Klicic, D. T. Mainz, M. P. Repasky, E. H. Knoll, M. Shelley, J. K. Perry, D. E. Shaw, P. Francis and P. S. Shenkin, *J. Med. Chem.*, 2004, **47**, 1739-1749.
35. W. Sherman, T. Day, M. P. Jacobson, R. A. Friesner and R. Farid, *J. Med. Chem.*, 2006, **49**, 534-553.
36. W. Sherman, S. Beard Hege and R. Farid, *Chem. Biol. Drug Des.*, 2006, **67**, 83-84.
37. J.-X. Lu, W. Qiang, W.-M. Yau, Charles D. Schwieters, Stephen C. Meredith and R. Tycko, *Cell*, 2013, **154**, 1257-1268.
38. T. Lührs, C. Ritter, M. Adrian, D. Riek-Loher, B. Bohrmann, H. Döbeli, D. Schubert and R. Riek, *Proc. Natl. Acad. Sci. U S A.*, 2005, **102**, 17342-17347.
39. A. T. Petkova, W.-M. Yau and R. Tycko, *Biochemistry*, 2006, **45**, 498-512.
40. J.-P. Colletier, A. Laganowsky, M. Landau, M. Zhao, A. B. Soriaga, L. Goldschmidt, D. Flot, D. Cascio, M. R. Sawaya and D. Eisenberg, *Proc. Natl. Acad. Sci. USA.*, 2011, **108**, 16938-16943.
41. M. G. Savelieff, S. Lee, Y. Liu and M. H. Lim, *ACS Chem. Biol.*, 2013, **8**, 856-865.
42. D.-Y. Choi, Y.-J. Lee, J. T. Hong and H.-J. Lee, *Brain Res. Bull.*, 2012, **87**, 144-153.
43. K. K. Teng, J. M. Angelastro, M. E. Cunningham and L. A. Greene, in *Cell Biology (Third Edition)*, ed. J. E. Celis, Academic Press, Burlington, 2006, DOI: <https://doi.org/10.1016/B978-012164730-8/50022-8>, pp. 171-176.
44. M. Pandeewar, H. Khare, S. Ramakumar and T. Govindaraju, *RSC Adv.*, 2014, **4**, 20154-20163.

### Graphical Abstract

#### L-Dopa and dopamine conjugated naphthalenediimides modulate amyloid $\beta$ toxicity

Madhu Ramesh, Pandeewar Makam, Chandrashekar Voshavar, Harshavardhan Khare, Kolla Rajasekhar, Suryanarayanan Rao Ramakumar, Thimmaiah Govindaraju\*

We report amino acids, L-dopa and dopamine functionalised naphthalenediimides and the detailed *in silico* and *in vitro* study to identify potential multifunctional modulator of amyloid  $\beta$  toxicity.

